／
Article／Book Information

（　　）	
Title(English)	Prediction of Wind-Induced Response for Damped System with Frequency-Sensitivity
（　　）	，
Authors(English)	Chang Ting-Wei, Daiki Sato
／Citation	，　，，pp. 353-356
Citation(English)	，　，，pp. 353-356
／Pub. date	2021，3

Prediction of Wind-Induced Response for Damped System with Frequency-Sensitivity

構造－振動　　　　　　　　　　　　正会員 ○　張庭維[*1]　正会員　佐藤大樹[*2]

Wind excitation, VE damper, Frequency-sensitivity,
Prediction Method, Power Spectral Density

1. Introduction

The time history analysis on the viscoelastic (VE) damped systems is a stable and reliable method to obtain the wind-induced response. After considering the frequency-sensitivity of the VE damped systems (Sato et al. 2009 [1]), the spectral analysis in the frequency domain can be used to improve the prediction method of the wind-induced response. In addition, it is a significant process to verify the reliability of the prediction method. This paper compares the prediction method with the time history analysis results of 1st mode wind-induced response, including the mean component of displacement, the variance of the responses, and input energy among damped systems in different frequency-sensitive models, such as the fractional derivative (FD) system, Kelvin system, Maxwell system, 4-element system, and 6-element system.

2. Analytical Wind and Target Building

This study employed wind forces with a return period of 100 years. Wind force was determined by using a wind tunnel test [2]. The airflow in the experiment was determined by referring to the building design load in Japan [3] (terrain: III, directional angle: 0 degree). The design wind velocities of the 100-year-return period is 54.9 m/s. The number of data were 14,000 with the time step $\Delta t = 0.05$ sec, total time $T_a = 700$ sec.

Figure (1) shows the 1st mode wind force of 50 stories analytical wind force evaluated by a 10 waves of the ensemble average, including along-wind direction along with the across-wind direction. The unit of the y-axis is dimensionless.

Based on Fig. (1), the PSD of the along-wind has a high power of a wide-band at low frequency. In contrast, the PSD of the across-wind has a high power of a peak at the frequency of 0.1 Hz. Fig. (2a, b) shows one example of the 1st mode wind force in time history. However, to avoid the additional impulse of the along-wind by its mean component, the beginning (0 sec~50 sec) and the end (650sec~700 sec) of the wind force was modified.

The target building was a 200 m height with an aspect ratio of 4.0, whose $D=B$=50m. Table.1 indicated models for the analysis. It was divided into 3-groups (1H, 2H, and 3H) by natural periods of frame (T_1 =2, 4, and 6 sec). In addition, there were 3 kinds of damper (hard: 'H,' soft: 'S,' and weak: 'W') and 2 kinds of brace stiffness (hard: 'H' and soft: 'S') considered.

3. Spectral Analysis

The spectral analysis is a fast calculation method to make an inner product between the power spectral density of wind and the transfer function of systems, in the frequency domain. Then, using the inverse of Fourier transform to obtain the response in the time domain. In Section 3 discussed about the transfer function of different VE damped systems.
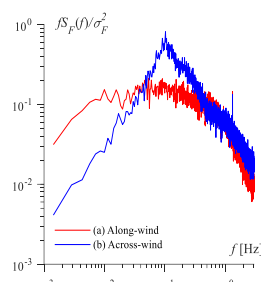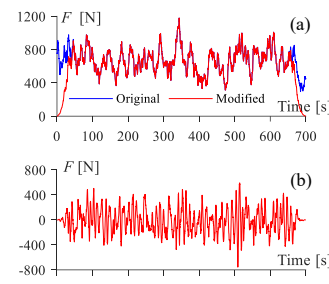

Fig. 1. PSD of Wind Excitation

Fig. 2. Time History of Wind Excitation
(a) Along-wind, (b) Across-wind

3.1. Analytical Models' Transfer Function

The transfer function of the 1st mode generalized VE damped system is given by Eq. (1). Where the storage stiffness K'_a, loss factor η'_a, and the loss stiffness K''_a of the added component are given by Eq. (2). However, the storage stiffness K'_d and loss factor η_d of the damper is different by different VE damped models (Table. 1), which discussed after Section 3.2.
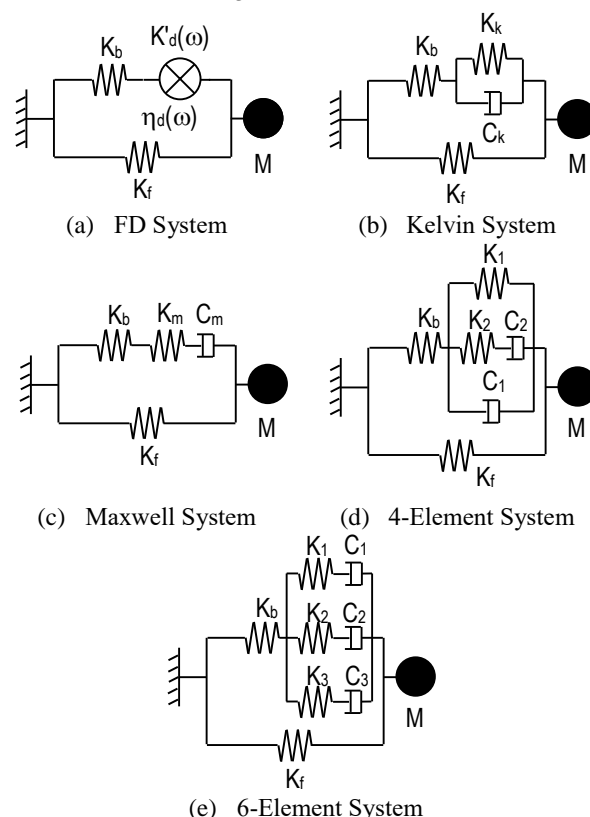

(a) FD System　　(b) Kelvin System

(c) Maxwell System　　(d) 4-Element System

(e) 6-Element System
Fig. 3. Viscoelastic Damped Systems

Prediction of Wind-Induced Response for Damped Systems with Frequency-Sensitivity　　Ting-Wei CHANG, Daiki SATO

$$H(i\omega) = \cfrac{1}{1 - \left(\cfrac{\omega}{\omega_0}\right)^2 + \cfrac{K'_a(\omega)}{K_f} + i\left(2\xi_0 \cfrac{\omega}{\omega_0} + \cfrac{K''_a(\omega)}{K_f}\right)} \cdot \cfrac{1}{K_f} \quad (1)$$

$$K'_a(\omega) = \frac{\{(1 + \eta_d^2(\omega))K'_d(\omega) + K_b\}K'_d(\omega)K_b}{(K'_d(\omega) + K_b)^2 + (\eta_d(\omega)K'_d(\omega))^2} \quad (2a)$$

$$\eta_a(\omega) = \frac{\eta_d(\omega)}{1 + (1 + \eta_d^2(\omega))K'_d(\omega)/K_b} \quad (2b)$$

$$K''_a(\omega) = K'_a(\omega) \cdot \eta_a(\omega) \quad (2c)$$

3.2. Fractional Derivative System

The parameters of the FD model (Fig. 3a) based on the dynamic feature of the FD model at the natural circular frequency ω_n. The storage stiffness $K'_d(\omega)$ and the loss factor $\eta_d(\omega)$ in the frequency domain are given by Eq. (3).

$$K'_d(\omega) = G\frac{1 + ab\omega^{2\alpha} + (a+b)\omega^\alpha \cos(\alpha\pi/2)}{1 + a^2\omega^{2\alpha} + 2a\omega^\alpha \cos(\alpha\pi/2)} \frac{A_s}{d} \quad (3a)$$

$$\eta_d(\omega) = \frac{(-a+b)\omega^\alpha \sin(\alpha\pi/2)}{1 + ab\omega^{2\alpha} + (a+b)\omega^\alpha \cos(\alpha\pi/2)} \quad (3b)$$

Where, A_s = laminations of VE damper, d = thickness of VE material lamination. In this paper, the 3M material ISD111 is adopted. Then, $G = 3.92 \times 10^4$, $a = 5.6 \times 10^{-5}$, $b = 2.10$, $\alpha = 0.558$.

3.3. Kelvin System

The storage stiffness $K'_d(\omega)$ and the loss factor $\eta_d(\omega)$ of the Kelvin system (Fig. 3b) in the frequency domain are given by Eq. (4).

$$K'_d(\omega) = K'_d = K_k \quad , \quad \eta_d(\omega) = C_k \cdot \omega/K_k \quad (4a, b)$$

3.4. Maxwell System

The storage stiffness $K'_d(\omega)$ and the loss factor $\eta_d(\omega)$ of the Maxwell system (Fig. 3c) in the frequency domain are given by Eq. (5).

$$K'_d(\omega) = \frac{K_m(C_m\omega)^2}{K_m^2 + (C_m\omega)^2}, \quad \eta_d(\omega) = \frac{K_m^2 C_m \omega}{K_m(C_m\omega)^2} \quad (5a, b)$$

3.5. 4-Element System

The storage stiffness $K'_d(\omega)$ and the loss factor $\eta_d(\omega)$ of the 4-Element system (Fig. 3d) in the frequency domain are given by Eq. (6).

$$K'_d = \frac{A_s}{d}\left[a_1 + \frac{a_2(b_2\omega)^2}{a_2^2 + (b_2\omega)^2}\right] \quad (6a)$$

$$K''_d = \frac{A_s}{d}\left[\frac{b_1\{a_2^2 + (b_2\omega)^2\}\omega + a_2^2(b_2\omega)}{a_2^2 + (b_2\omega)^2}\right] \quad (6b)$$

$$\eta_d(\omega) = \frac{K''_d(\omega)}{K'_d(\omega)} \quad (6c)$$

3.6. 6-Element System

The storage stiffness $K'_d(\omega)$ and the loss factor $\eta_d(\omega)$ of the 6-Element system (Fig. 3e) in the frequency domain are given by Eq. (7).

$$K'_d = \frac{A_s}{d}\left[\sum_i^3 \frac{a_i(b_i\omega)^2}{a_i^2 + (b_i\omega)^2}\right] \quad (7a)$$

$$\quad (7b)$$

$$\eta_d(\omega) = \frac{K''_d(\omega)}{K'_d(\omega)} \quad (7c)$$

4. Prediction of Mean Component of Displacement

The 1st mode mean component in the displacement response of the systems subjected to the along-wind were evaluated by using the 1st mode stationary stiffness $\overline{K'}$ and the average wind force $\overline{F}$. The stationary stiffness $\overline{K'}$ is derived from Eq. (8) to Eq. (10), which was at the condition for the frequency equal to zero. Besides, the mean component of the displacement at top of the building comes from the Hook's theory, which is given by Eq. (11).

$$\overline{K'_d} = \lim_{\omega \to 0} K'_d(\omega) = GA_s/d, \quad \lim_{\omega \to 0} \eta_d(\omega) = 0 \quad (8)$$

$$\overline{K'_a} = K_b \cdot \overline{K'_d}/(K_b + \overline{K'_d}) \quad (9)$$

$$\overline{K'} = K_f \cdot \overline{K'_a} \quad (10)$$

$$\overline{x}_i = \frac{\overline{K'}}{\overline{F}}\emptyset_{i,1} \quad (11)$$

Figure (4) shows the comparison of mean component in the along-wind displacement response at top of the building by time history analysis and by the prediction method of spectral analysis for the FD system, Kelvin system, Maxwell system, 4-Element system, and 6-Element system. Besides, the mean component of displacement response for the prediction method of spectral analysis had high accuracy with that of analysis.
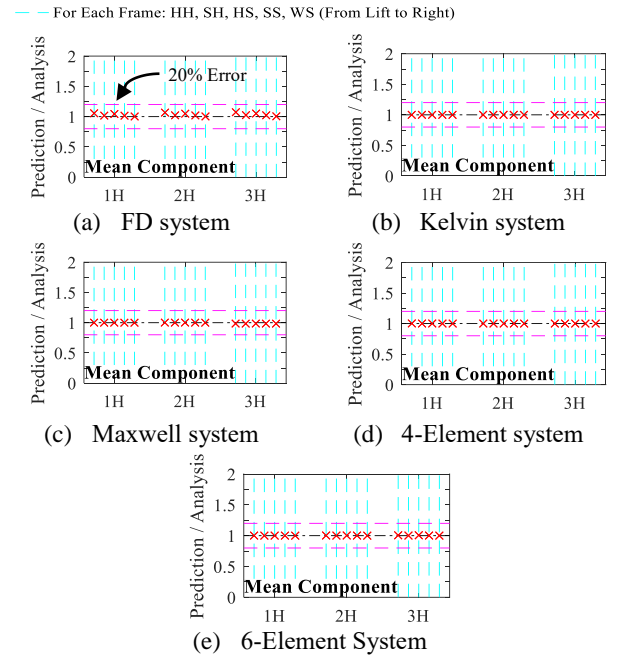

Fig. 4. Comparison of mean component in the along-wind displacement response at top of the building

5. Prediction of Deviation in the PSD

Based on the prediction method by spectral analysis, the PSD of the 1st mode displacement, velocity, and acceleration response at i^{th} floor of the building are given by Eq. (12).

$$S_{D,i}(\omega) = \emptyset_{i,1}^2 |H(i\omega)|^2 S_{F,1}(\omega) \quad (12a)$$

$$S_{v,i}(\omega) = \emptyset_{i,1}^2 |\dot{H}(i\omega)|^2 S_{F,1}(\omega) \quad (12b)$$

$$S_{A,i}(\omega) = \emptyset_{i,1}^2 |\ddot{H}(i\omega)|^2 S_{F,1}(\omega) \quad (12c)$$

Where,

$\emptyset_{i,1}$ = 1st mode's eigenvector of ith floor.

$H(i\omega)$ = transfer function, which is given by Eq. (1).

$$\dot{H}(i\omega) = i2\pi\omega H(i\omega), \tag{13}$$

$$\ddot{H}(i\omega) = -(2\pi\omega)^2 H(i\omega). \tag{14}$$

$S_{F,1}(\omega)$= PSD of the 1st mode wind force.

In addition, the 1th mode variance of the displacement $\sigma_{D,i}^2$, velocity $\sigma_{v,i}^2$, and acceleration $\sigma_{A,i}^2$ at ith floor of the building come from the integral of the PSD of $S_{D,i}$, $S_{V,i}$, and $S_{A,i}$, which are given by Eq. (15).

$$\sigma_{D,i}^2 = \int_0^\infty S_{D,i}(\omega)d\omega, \tag{15a}$$

$$\sigma_{v,i}^2 = \int_0^\infty S_{v,i}(\omega)d\omega \tag{15b}$$

$$\sigma_{A,i}^2 = \int_0^\infty S_{A,i}(\omega)d\omega \tag{15c}$$

Figure. (5) shows the comparison of variance of along-wind and across-wind response at the top floor in displacement, velocity, and acceleration response by time history analysis and by the prediction method of spectral analysis for the FD system, Kelvin system, Maxwell system, 4-Element system, and 6-Element system. The variances of the prediction method of spectral analysis had good agreement with that of analysis among displacement, velocity, and acceleration.

6.   Prediction of Input Energy

The prediction of the 1st mode input energy E_{input} for 10 minutes wind excitation is obtained by Eq. (16), proposed by Yoshie et al (2003) [4].

$$E_{input} = t_a \int_0^\infty R_e[\dot{H}(\omega)] \cdot S_{F,1}(\omega)d\omega \tag{16}$$

Where,

$\emptyset_{i,1}$= 1st mode's eigenvector of ith floor.

$R_e[\dot{H}(\omega)] = $ real part of transfer function in velocity (Eq. 13).

$S_{F,1}(\omega)$= PSD of the 1st mode wind force, which is evaluated by a 10 waves of the ensemble average.

In other hands, the analysis solution of input energy E_{input} for t_a minutes wind excitation is given by Eq. (17).

$$E_{input} = \int_{t_0}^{t_a} \dot{x}(t) \cdot F(t)dt \tag{17}$$

Where,

$\dot{x}(t) = $ response of velocity at 1st mode.

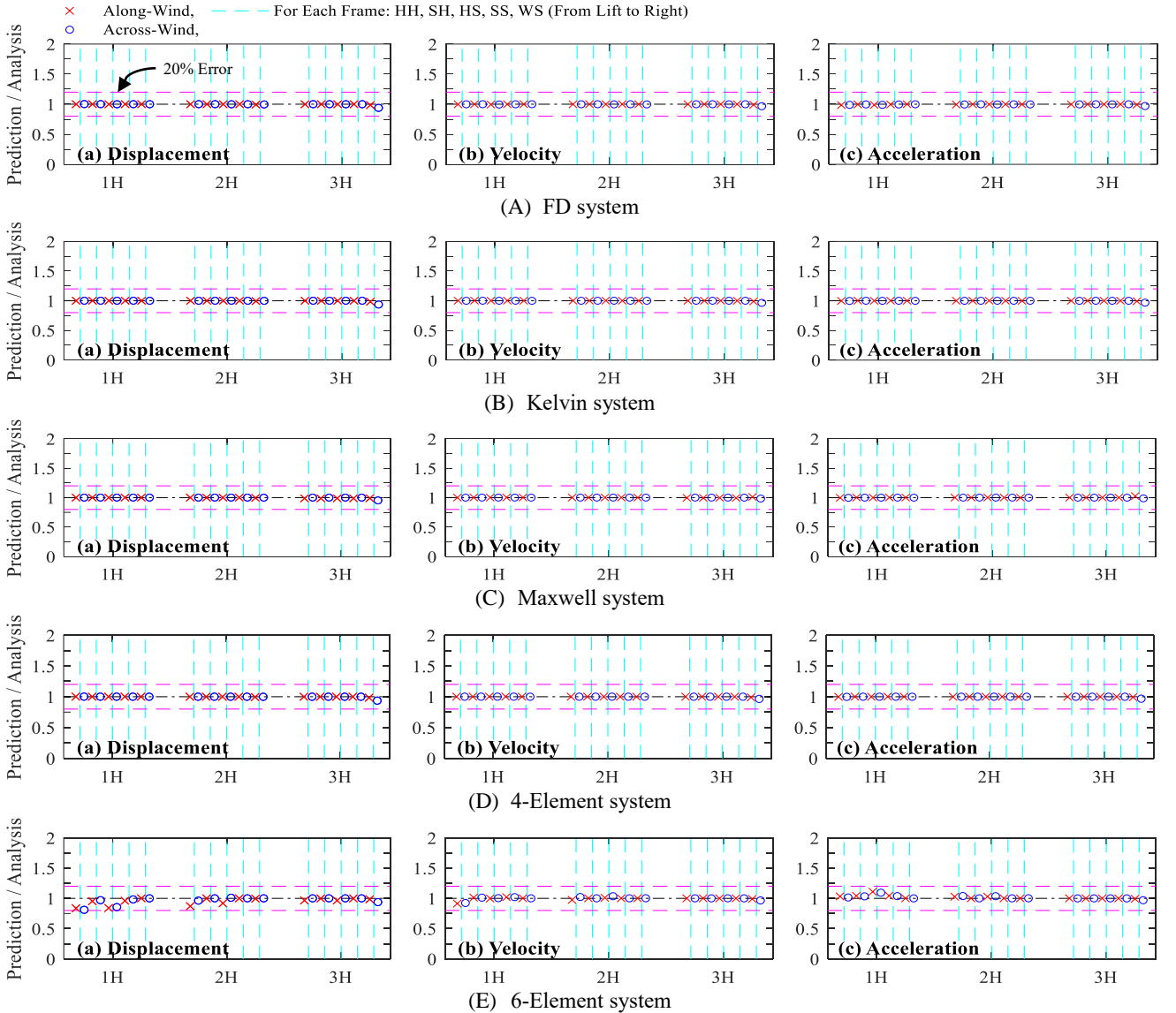$F(t)$= 1st mode wind force in time domain.

Fig. 5. Comparison of variance of along-wind displacement, velocity, and acceleration response at the top of building

Figure (6) shows the comparison of the 10 minutes (t_a=600 sec) input energy between the prediction (Eq. 16) and analysis (Eq. 17), which presents a high accuracy.

7.   Conclusions

This paper presented the accuracy of the prediction method, which having good agreement with time history analysis subjected to both along- and across-wind force, including the mean component of displacement response of the prediction method, the variance of the prediction method, and the 1st mode input energy.

Acknowledgement

Reference

[1] D. Sato, K. Kasai, and T. Tamura. Influence of frequency sensitivity of viscoelastic damper on wind-induced response. (Transactions of AIJ), 74(635), 75-82, 2009 [in Japanese].

[2] Marukawa H, Ohkuma T, Kitimura H, Yoshie K, Tsurumi T, Sato D. 20097 energy input of local wind forces for high-rise building based on wind tunnel test: Part. 2 local wind force characteristics of rectangular high-rise buildings, no. 2010. Architectural Institute of Japan; 2010. [in Japanese].

[3] Architectural Institute of Japan, AIJ Recommendation for Loads on Buildings, Architectural Institute of Japan, 2015.

[4] K.Yoshie, H. Kitamura, T. Ohkuma. A study of wind-induced energy input to an elasto-plastic structure. (Transactions of AIJ), No.572, 31-38, 2003 [in Japanese].
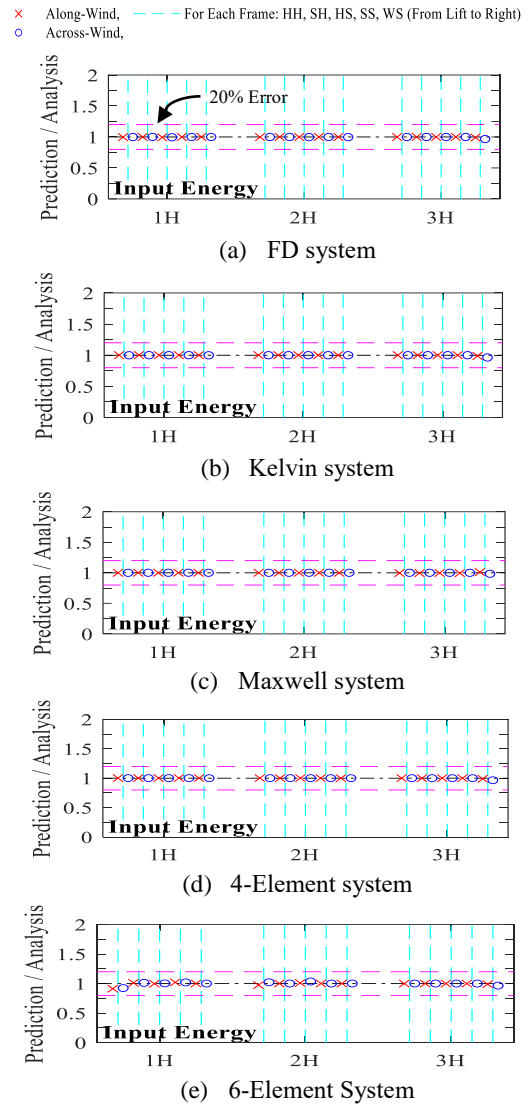

(a)   FD system

(b)   Kelvin system

(c)   Maxwell system

(d)   4-Element system

(e)   6-Element System

Fig. 6. Comparison of input energy

Table.1. Analytical VE damped models list

K_f (N/m)	Brace	K_b (N/m)	Damper	f_n (Hz)	ξ_n	FD system	Kelvin system	Maxwell system	4-Element system	6-Element system
9.870	Hard	∞	Hard	0.866	0.311	Fd1H-HH	Kv1H-HH	Mw1H-HH	Fe1H-HH	Se1H-HH
			Soft	0.592	0.126	Fd1H-SH	Kv1H-SH	Mw1H-SH	Fe1H-SH	Se1H-SH
	Soft	29.61	Hard	0.777	0.121	Fd1H-HS	Kv1H-HS	Mw1H-HS	Fe1H-HS	Se1H-HS
			Soft	0.588	0.098	Fd1H-SS	Kv1H-SS	Mw1H-SS	Fe1H-SS	Se1H-SS
			Weak	0.512	0.020	Fd1H-WS	Kv1H-WS	Mw1H-WS	Fe1H-WS	Se1H-WS
2.467	Hard	∞	Hard	0.433	0.281	Fd2H-HH	Kv2H-HH	Mw2H-HH	Fe2H-HH	Se2H-HH
			Soft	0.296	0.112	Fd2H-SH	Kv2H-SH	Mw2H-SH	Fe2H-SH	Se2H-SH
	Soft	7.401	Hard	0.385	0.113	Fd2H-HS	Kv2H-HS	Mw2H-HS	Fe2H-HS	Se2H-HS
			Soft	0.293	0.088	Fd2H-SS	Kv2H-SS	Mw2H-SS	Fe2H-SS	Se2H-SS
			Weak	0.257	0.020	Fd2H-WS	Kv2H-WS	Mw2H-WS	Fe2H-WS	Se2H-WS
1.097	Hard	∞	Hard	0.289	0.261	Fd3H-HH	Kv3H-HH	Mw3H-HH	Fe3H-HH	Se3H-HH
			Soft	0.197	0.103	Fd3H-SH	Kv3H-SH	Mw3H-SH	Fe3H-SH	Se3H-SH
	Soft	3.290	Hard	0.256	0.107	Fd3H-HS	Kv3H-HS	Mw3H-HS	Fe3H-HS	Se3H-HS
			Soft	0.195	0.081	Fd3H-SS	Kv3H-SS	Mw3H-SS	Fe3H-SS	Se3H-SS
			Weak	0.172	0.020	Fd3H-WS	Kv3H-WS	Mw3H-WS	Fe3H-WS	Se3H-WS

*1 東京工業大学 大学院生   Graduate Student, Tokyo Institute of Technology
*2 東京工業大学 准教授・博士（工学）   Assoc. Prof., Tokyo Institute of Technology, Dr. Eng.